**Advanced Steel Construction** – Vol. 20 No. 4 (2024) 424–436
**DOI:**10.18057/IJASC.2024.20.4.10



# METAL BEAMS SUSCEPTIBLE TO OUT-OF-PLANE INSTABILITY DUE TO COMBINED COMPRESSION AND BENDING WITH GEOMETRIC IMPERFECTIONS

Antonio Aguero [1, *], Ana Almerich-Chulia [1], Yvona Kolekova [2] and Pedro Martin-Concepcion [1]

[1] *Dept. of Continuous Medium Mechanics and Theory of Structures, Universitat Politècnica de València, c/Camino de Vera s/n, 46022 Valencia, Spain*

[2] *Dept. of Structural Mechanics, Faculty of Civil Engineering, Slovak University of Technology in Bratislava, Bratislava, Slovak Republic*

** (Corresponding author: E-mail: anagra@mes.upv.es)*

**A B S T R A C T**

The parts of the second generation of Eurocodes are continuously published. The full set of the 2nd generation of these new European standards consists of 68 parts of Eurocodes, 15 Technical Specifications and 5 Technical Reports and they will all be available in 2028. The aim of the paper is to bridge the gap concerning one of the newest and the most complex UGLI (Unique Global and Local Initial) imperfection methods. According to EN 1993-1-1:2022, ultimate limit state design checks may be carried out using methods of analysis named hereafter as M0, M1, M2, M3, M4, M5 or EM. Both Eurocodes EN 1993-1-1:2022 and EN 1999-1-1:2023 state, as an alternative that to sway and equivalent bow imperfection the new UGLI imperfection method may be employed for global and member analyses. In previous papers, plane stability was mostly investigated. The method presented in this paper enables the computing of the amplitude of the initial imperfection of elements under compression bending susceptible to out-of-plane buckling, and is a generalization of Eurocode rules, which is valid only for members under compression. This work is a continuation of a previous work by Agüero, in which the way to compute the UGLI imperfection was generalized for flexural torsional buckling due to compression and lateral torsional buckling due to bending. Some examples are presented to show the agreement with GMNIA (Geometrical material nonlinear analysis of imperfect structures), tests and proposals with codes.

**A R T I C L E  H I S T O R Y**

Received: 22 April 2024
Revised: 21 October 2024
Accepted: 9 November 2024

**K E Y W O R D S**

Out-of-plane instability;
EN 1993-1-1:2005;
EN 1993-1-1:2022;
Equivalent UGLI imperfection;
Imperfection shapes;
Imperfection amplitudes



## 1. Introduction

EN 1993-1-1 [1] and EN 1999-1-1 [2] outline the design of metal structures with compression elements, and imperfections and their effects must be considered.

1-Indirectly by performing a linear analysis, plus interaction formulae. This method includes nonlinearity using buckling curves to obtain reduction factor $\chi$.

2-Directly by including imperfections in the nonlinear analysis.

This involves geometrical imperfections and residual stresses. The imperfections below must be contemplated: a) global imperfections for bracing systems and frames; b) local imperfections for individual members; c) the structure's elastic critical buckling mode $\eta_{cr}$ shape in line with clauses 5.3.2(11) of [1] and [2], 7.3.6 of [4] as the geometrical equivalent UGLI (Unique Global and Local Initial) imperfection.

Below are some methods that allow the buckling resistance of sensitive beams to lateral torsional buckling according to [1], [2], [3] and [4] to be obtained:

• The indirect method involves a linear analysis. It includes not only geometrical, but also material nonlinearity and imperfections, by buckling curves to acquire reduction factor $\chi_{LT}$ according to clause 6.3 of [1].

• The direct method involves a second-order analysis with equivalent geometric imperfections.

In accordance with clauses 5.3.4(3) in [1,2] and 7.3.4(3) in [4], "Taking account of lateral torsional buckling of a member in bending the imperfections may be adopted as $k \cdot e_0$, where $e_0$ is the equivalent initial bow imperfection of the weak axis of the profile considered. In general, additional torsional imperfection does not need to be allowed for. The value k = 0.5 is recommended. The National Annex may choose the value of k."

In line with 7.3.3.2 in [3], "For a 2nd-order analysis, by taking into account the lateral torsional buckling of a member in bending, the equivalent imperfection may be determined according to (7.11), where $e_{0,LT}$ is the equivalent bow imperfection about the weak axis of the considered profile. In general, additional torsional imperfection may be neglected".

Here a numerical method permits the equivalent initial imperfection to be obtained for beams with a doubly symmetric section susceptible to lateral torsional buckling.

For the elements that form part of the bending-compression combination, and with out-of-plane instability, clauses 6.3.3 and 6.3.4 in [1,2], or clauses 8.3.3 and 8.3.4 in [4], come into play. Interaction formula or a nonlinear analysis of the imperfect structure may be used.

It is possible to express imperfection in the form of single imperfection, as in the structure's buckling mode $\eta_{cr}(x)$ (clauses 5.3.2 (11) in [1-2], 7.3.6(1) in [3], 7.3.2(11) in [4]). It is known as the geometrical equivalent UGLI (Unique Global and Local Initial) imperfection. See Chladný et al. [5,6,7] for a complete description.

The proposals of [1-4] fall in line with "(1)", with flexural buckling occurring around a strong axis due to compression.

Imperfections are generally expressed as:

$$\{\eta_{init}(x)\} = \eta_0 \{\eta_{cr}(x)\}$$
$$\eta_{init}(x) = \left( \frac{\alpha(\bar{\lambda}-\bar{\lambda}_0)}{\bar{\lambda}^2} \frac{1-\dfrac{\bar{\lambda}^2\cdot\chi}{\gamma_{M1}}}{1-\bar{\lambda}^2\cdot\chi} \frac{f_y}{E\left(\dfrac{I}{W}\dfrac{d^2\eta_{cr}}{dx^2}\right)} \right)_{X_{cr}} \tag{1}$$
$$\eta_{cr}(x) = \eta_0 \cdot \eta_{cr}(x)$$

For flexural buckling around a strong axis:

$$\eta_{init,w}(x) = \left( \frac{\alpha(\bar{\lambda}-\bar{\lambda}_0)}{\bar{\lambda}^2} \frac{1-\dfrac{\bar{\lambda}^2\cdot\chi}{\gamma_{M1}}}{1-\bar{\lambda}^2\cdot\chi} \frac{f_y}{E\left(\dfrac{I_y}{W_y}\dfrac{d^2\eta_{cr,w}}{dx^2}\right)} \right)_{X_{cr}} \tag{2}$$
$$\eta_{cr,w}(x) = \eta_0 \cdot \eta_{cr,w}(x)$$

For flexural buckling around a weak axis:

$$\eta_{init,v}(x) = \left( \frac{\alpha(\bar{\lambda}-\bar{\lambda}_0)}{\bar{\lambda}^2} \frac{1-\dfrac{\bar{\lambda}^2\cdot\chi}{\gamma_{M1}}}{1-\bar{\lambda}^2\cdot\chi} \frac{f_y}{E\left(\dfrac{I_z}{W_z}\dfrac{d^2\eta_{cr,v}}{dx^2}\right)} \right)_{X_{cr}} \tag{3}$$
$$\eta_{cr,v}(x) = \eta_0 \cdot \eta_{cr,v}(x)$$

No iteration is needed for prismatic elements with uniform axial forces. The critical section occurs where the curvature is maximum. Iteration is needed in the majority of practical cases.

See Chladný et al. [5-7] for further generalization. Flexural buckling takes place around both the axes as so "(4)".

$$\begin{Bmatrix} \eta_{init,v}(x) \\ \eta_{init,w}(x) \end{Bmatrix} = \left( \frac{\alpha(\bar{\lambda}-\bar{\lambda}_0)}{\bar{\lambda}^2} \frac{1-\frac{\bar{\lambda}^2\cdot\chi}{\gamma_{M1}}}{1-\bar{\lambda}^2\cdot\chi} \frac{f_y}{E\left(\frac{I_z}{W_z}\left|\frac{d^2\eta_{cr,v}}{dx^2}\right| + \frac{I_y}{W_y}\left|\frac{d^2\eta_{cr,w}}{dx^2}\right|\right)} \right)_{X_{cr}} \tag{4}$$
$$\begin{Bmatrix} \eta_{cr,v}(x) \\ \eta_{cr,w}(x) \end{Bmatrix} = \eta_0 \cdot \begin{Bmatrix} \eta_{cr,v}(x) \\ \eta_{cr,w}(x) \end{Bmatrix}$$

Simplifying “(2)”, “(3)” and “(4)” can be done by discarding partial safety factor $\gamma_{M1}$.

This is not advisable because it destroys the method’s basic feature and the results differ from those obtained for the equivalent member method for $N_{Ed} = N_{b,Rd}$.

The novel methodology has emerged in recent times in some publications, with examples displaying how to achieve flexural buckling resistance for members with arch structures, nonuniform cross-sections and nonuniform axial forces [8-11]. According to [8], the amplitude of such imperfection offers a different way by comparing it to Chladný`s method.

Agüero et al. [9,10] offer a generalization of flexural torsional buckling owing to compression, in which an imperfect structure analysis is done as “(5)”.

$$\begin{Bmatrix} \eta_{init,v}(x) \\ \eta_{init,w}(x) \\ \eta_{init,\theta x}(x) \end{Bmatrix} =$$
$$\left( \frac{\alpha(\bar{\lambda}-\bar{\lambda}_0)}{\bar{\lambda}^2} \frac{1-\frac{\bar{\lambda}^2\cdot\chi}{\gamma_{M1}}}{1-\bar{\lambda}^2\cdot\chi} \frac{f_y}{E\left(\frac{I_z}{W_z}\frac{d^2\eta_{cr,v}}{dx^2} + \frac{I_y}{W_y}\frac{d^2\eta_{cr,w}}{dx^2} + \frac{I_w}{W_{Bi}}\frac{d^2\eta_{cr,\theta x}}{dx^2}\right)} \right)_{X_{cr}} \tag{5}$$
$$\begin{Bmatrix} \eta_{cr,v}(x) \\ \eta_{cr,w}(x) \\ \eta_{cr,\theta x}(x) \end{Bmatrix} = \eta_0 \cdot \begin{Bmatrix} \eta_{cr,v}(x) \\ \eta_{cr,w}(x) \\ \eta_{cr,\theta x}(x) \end{Bmatrix}$$

The next equation can be applied in accordance with clause 8.3.1.4 [3] for doubly symmetric I- and H-sections.

$$\begin{Bmatrix} \eta_{init,v}(x) \\ \eta_{init,w}(x) \\ \eta_{init,\theta x}(x) \end{Bmatrix} =$$
$$\left( \left(\frac{\bar{\lambda}_{TF}}{\bar{\lambda}_z}\right)^2 \frac{\alpha_{TF}(\bar{\lambda}_z-\bar{\lambda}_0)}{\bar{\lambda}_{TF}^{\,2}} \frac{1-\frac{\bar{\lambda}_{TF}^{\,2}\cdot\chi}{\gamma_{M1}}}{1-\bar{\lambda}_{TF}^{\,2}\cdot\chi} \frac{f_y}{E\left(\frac{I_z}{W_z}\frac{d^2\eta_{cr,v}}{dx^2} + \frac{I_y}{W_y}\frac{d^2\eta_{cr,w}}{dx^2} + \frac{I_w}{W_{Bi}}\frac{d^2\eta_{cr,\theta x}}{dx^2}\right)} \right)_{X_{cr}} \tag{6}$$
$$\begin{Bmatrix} \eta_{cr,v}(x) \\ \eta_{cr,w}(x) \\ \eta_{cr,\theta x}(x) \end{Bmatrix} = \eta_0 \cdot \begin{Bmatrix} \eta_{cr,v}(x) \\ \eta_{cr,w}(x) \\ \eta_{cr,\theta x}(x) \end{Bmatrix}$$

Agüero et al. [9,10] (Fig. 4) present another generalization for lateral torsional buckling, which describes the imperfect structure analysis as “(7)”.

$$\begin{Bmatrix} \eta_{init,v}(x) \\ \eta_{init,\theta x}(x) \end{Bmatrix} =$$
$$\left( \frac{\alpha_{LT}(\bar{\lambda}_{LT}-\bar{\lambda}_{LT,0})}{\bar{\lambda}_{LT}^{\,2}} \frac{1-\frac{\bar{\lambda}_{LT}^{\,2}\cdot\chi_{LT}}{\gamma_{M1}}}{1-\beta\cdot\bar{\lambda}_{LT}^{\,2}\cdot\chi_{LT}} \frac{f_y}{E\left(\frac{I_z}{W_z}\left|\frac{d^2\eta_{cr,v}}{dx^2}\right| + \frac{I_w}{W_{Bi}}\left|\frac{d^2\eta_{cr,\theta x}}{dx^2}\right|\right)} \right)_{X_{cr}} \tag{7}$$
$$\begin{Bmatrix} \eta_{cr,v}(x) \\ \eta_{cr,\theta x}(x) \end{Bmatrix} = \eta_0 \cdot \begin{Bmatrix} \eta_{cr,v}(x) \\ \eta_{cr,\theta x}(x) \end{Bmatrix}$$

The curvatures for doubly symmetric sections are taken as the absolute value.

According to clause 8.3.2.3 in [3] for not only fork supports at both ends, but also doubly symmetric I and H-sections, the next equation may apply, where $f_M = 1$ (Table 8.6 of [3]):

$$\begin{Bmatrix} \eta_{init,v}(x) \\ \eta_{init,\theta x}(x) \end{Bmatrix} =$$
$$\left( \left(\frac{\bar{\lambda}_{LT}}{\bar{\lambda}_z}\right)^2 \frac{\alpha_{LT}(\bar{\lambda}_z-\bar{\lambda}_{LT,0})}{\bar{\lambda}_{LT}^{\,2}} \frac{1-\frac{\bar{\lambda}_{LT}^{\,2}\cdot\chi_{LT}}{\gamma_{M1}}}{1-\bar{\lambda}_{LT}^{\,2}\cdot\chi_{LT}} \frac{f_y}{E\left(\frac{I_z}{W_z}\left|\frac{d^2\eta_{cr,v}}{dx^2}\right| + \frac{I_w}{W_{Bi}}\left|\frac{d^2\eta_{cr,\theta x}}{dx^2}\right|\right)} \right)_{X_{cr}} \tag{8}$$
$$\begin{Bmatrix} \eta_{cr,v}(x) \\ \eta_{cr,\theta x}(x) \end{Bmatrix} = \eta_0 \cdot \begin{Bmatrix} \eta_{cr,v}(x) \\ \eta_{cr,\theta x}(x) \end{Bmatrix}$$

Bijlaard et al. [11] and Wieschollek et al. [12] generalize the equation found in Eurocodes [1,3] for lateral torsional buckling cases, when cross-section flanges are taken as sensitive members to flexural buckling and under compression by applying Chladný’s method. Papp [13] solves buckling under bending and compression, and Trahair [14] contemplates beam column behavior.

In the event of out-of-plane instability caused by compression and bending in line with clause 6.3.4 in [1], the most recent proposals can be generalized by applying exactly the same method as that depicted in [9,10]. A similar equation to former ones is obtained:

$$\begin{Bmatrix} \eta_{init,v}(x) \\ \eta_{init,\theta x}(x) \end{Bmatrix} =$$
$$\left( \frac{\alpha^*(\bar{\lambda}_{op}-\bar{\lambda}_{op,0})}{\bar{\lambda}_{op}^{\,2}} \frac{1-\frac{\bar{\lambda}_{op}^{\,2}\cdot\chi_{op}}{\gamma_{M1}}}{1-\bar{\lambda}_{op}^{\,2}\cdot\chi_{op}} \frac{f_y}{E\left(\frac{I_z}{W_z}\left|\frac{d^2\eta_{cr,v}}{dx^2}\right| + \frac{I_w}{W_{Bi}}\left|\frac{d^2\eta_{cr,\theta x}}{dx^2}\right|\right)} \right)_{X_{cr}} \tag{9}$$
$$\begin{Bmatrix} \eta_{cr,v}(x) \\ \eta_{cr,\theta x}(x) \end{Bmatrix} = \eta_0 \cdot \begin{Bmatrix} \eta_{cr,v}(x) \\ \eta_{cr,\theta x}(x) \end{Bmatrix}$$

where:

$$\bar{\lambda}_{op} = \sqrt{\frac{\alpha_{ult,k}}{\alpha_{cr,op}}} \tag{10}$$

$$\frac{1}{\alpha_{ult,k}} = \left(\frac{N_{Ed}}{N_{Rk}} + \frac{M_{y,Ed}}{M_{y,Rk}}\right)_{X_{cr}} \tag{11}$$

The critical section is accomplished as in Agüero [9,10].

## 2. Research significance

This article reports innovation by accomplishing imperfection for beam columns with out-of-plane instability that form part of the bending-compression combination when only bending “(9)” exists and is the equivalent to “(7)”. The means to do so is coherent with the authors’ former proposals.

The inclusions of the equivalent geometric imperfections in nonlinear analyses offer these advantages:

- At the section level, buckling appears as further internal forces and displacements. Equilibrium and compatibility equations are checked rather than stability checks, which are carried out on members and diminish their strength.
- A global issue is the buckling problem. It is analyzed by bearing in mind structures’ members interaction, and not only that of members under compression. Here secondary internal forces emerge on either tension members or stabilizing beams.

## 3. The method followed to know the amplitude of imperfection

Buckling shape is scaled with a maximum value of 1.0; e.g. $\max[\eta_{cr,v}(x)] = 1.0$. $\eta_0$, which means the amplitude of imperfection in the shear center.

$$\begin{aligned} \eta_0 &= \eta_{init,v}(x_{\max,v}) = \max\left(\eta_{init,v}(x)\right) = \max\left(\eta_0\eta_{cr,v}(x)\right) \\ \eta_{init,\theta x}(x_{\max,\theta x}) &= \max\left(\eta_{init,\theta x}(x)\right) = \max\left(\eta_0\eta_{cr,\theta x}(x)\right) \end{aligned} \tag{12}$$

To know imperfection, the next four steps are taken:

**Step 1:** compute buckling load αcr and buckling shape $\eta_{cr}(x)$, both of which can be calculated by the FEM (Finite Element Method).

**Step 2:** compute not only the bending moments around weak axes z, but also the bi-moments associated with the buckling mode. Internal bending/torsion forces are accomplished as so:

$$\begin{aligned} M_{z\eta}(x) &= EI_z \frac{d^2\eta_{cr,v}}{dx^2} \\ B_\eta(x) &= EI_w \frac{d^2\eta_{cr,\theta x}}{dx^2} \end{aligned} \tag{13}$$

Relevant stresses are computed from this equation:

$$\sigma_{Mz}(x)+\sigma_B(x) = \frac{EI_z}{W_z}\frac{d^2\eta_{cr,v}}{dx^2} + \frac{EI_w}{W_B}\frac{d^2\eta_{cr,\theta x}}{dx^2} \tag{14}$$

**Step 3:** The first calculation iteration applies the initial guess:

$$\begin{aligned} \alpha_{ult,1} &= \min\left(\frac{1}{\dfrac{N}{A\cdot f_y}+\dfrac{M_y}{W_y\cdot f_y}}\right) \\ \bar{\lambda}_{op,1} &= \sqrt{\frac{\alpha_{ult,1}}{\alpha_{cr}}} \rightarrow \chi_{op,1} \rightarrow \alpha_{b,1} = \frac{\alpha_{ult,1}\cdot\chi_{op,1}}{\gamma_{M1}} \end{aligned} \tag{15}$$

To acquire the maximum in"(14)", a better initial guess can be contemplated. To reach cross-section resistance $\alpha_{b,1}$ at the moment when the buckling load level is achieved, imperfection (scale factor $\Omega_1(x)$) needs to be computed in all the sections.

$$\frac{f_y}{\gamma_{M0}} = \frac{N_{Ed}\cdot\alpha_{b,1}}{A} + \frac{M_{y,Ed}\cdot\alpha_{b,1}}{W_y} + \frac{\Omega_1(x)}{\left(\dfrac{\alpha_{cr}}{\alpha_{b,1}}-1\right)}\left(E\left(\frac{I_z}{W_z}\frac{d^2\eta_{cr,v}}{dx^2}+\frac{I_w}{W_B}\frac{d^2\eta_{cr,\theta x}}{dx^2}\right)\right) \tag{16}$$

$$\Omega_1(x) = \frac{\left(\dfrac{f_y}{\gamma_{M0}} - \dfrac{N_{Ed}\cdot\alpha_{b,1}}{A} - \dfrac{M_{y,Ed}\cdot\alpha_{b,1}}{W_y}\right)\left(\dfrac{\alpha_{cr}}{\alpha_{b,1}}-1\right)}{E\left(\dfrac{I_z}{W_z}\dfrac{d^2\eta_{cr,v}}{dx^2}+\dfrac{I_w}{W_B}\dfrac{d^2\eta_{cr,\theta x}}{dx^2}\right)} \tag{17}$$

The purpose of the first iteration is to obtain the minimum of these scale factors; e.g., $\eta_{0,1}$ occurs at critical section $x_{cr,1}$.

$$\eta_{0,1} = \min(\Omega_1(x)) = \Omega_1\left(x_{cr,1}\right) \tag{18}$$

**Step 4:** For the second iteration:

$$\begin{aligned} \alpha_{ult,2} &= \left(\frac{1}{\dfrac{N}{A\cdot f_y}+\dfrac{M_y}{W_y\cdot f_y}}\right)\cdot x_{cr} \rightarrow \bar{\lambda}_{op,2} = \sqrt{\frac{\alpha_{ult,2}}{\alpha_{cr}}} \rightarrow \chi_{op,2} \rightarrow \\ \alpha_{b,1} &= \frac{\alpha_{ult,1}\cdot\chi_{op,2}}{\gamma_{M1}} \end{aligned} \tag{19}$$

Then calculate utilization factor U(x) along the beam:

$$\begin{aligned} &U_{N+My+Mz+Bi}(x) = \\ &= \left|\frac{N_{Ed}\cdot\alpha_{b,2}}{A\dfrac{f_y}{\gamma_{M0}}}\right| + \left|\frac{M_{y,Ed}\cdot\alpha_{b,2}}{W_y\dfrac{f_y}{\gamma_{M0}}}\right| + \\ &+\left[\frac{\eta_{0,1}}{\left(\dfrac{\alpha_{cr}}{\alpha_{b,2}}-1\right)}\frac{EI_z\left|\dfrac{d^2\eta_{cr,v}}{dx^2}\right|}{W_z\dfrac{f_y}{\gamma_{M0}}}\right] + \left[\frac{\eta_{0,1}}{\left(\dfrac{\alpha_{cr}}{\alpha_{b,2}}-1\right)}\frac{EI_w\left|\dfrac{d^2\eta_{cr,\theta x}}{dx^2}\right|}{W_B\dfrac{f_y}{\gamma_{M0}}}\right] \end{aligned} \tag{20}$$

The maximum utilization for doubly symmetric sections is acquired as the sum of the absolute values of the partial utilizations.

Compute the next critical section $x_{cr,2}$. Utilization factor U is the maximum:

$$\max(U_{N+M_y+M_z+B}(x)) = U_{N+M_y+M_z+B}(x_{cr,2}) \tag{21}$$

Let's assume that the critical section is the same as in the previous iteration event. In this case, critical section xcr is found and, as a consequence, it also takes the initial imperfection amplitude η0 value toward initial imperfection.

$$\{\eta_{init}\} = \eta_0\left(\eta_{cr}\right) \tag{22}$$

If the critical section's location is different from the one before, another iteration is necessary in Step 4 until the critical section's position is known:

$$\eta_{0,2} = \left(\frac{\left(\dfrac{f_y}{\gamma_{M0}} - \dfrac{N_{Ed}\cdot\alpha_{b,2}}{A} + \dfrac{M_{y,Ed}\cdot\alpha_{b,2}}{W_y}\right)\left(\dfrac{\alpha_{cr}}{\alpha_{b,2}}-1\right)}{E\left(\dfrac{I_z}{W_z}\dfrac{d^2\eta_{cr,v}}{dx^2}+\dfrac{I_w}{W_B}\dfrac{d^2\eta_{cr,\theta x}}{dx^2}\right)}\right)_{x_{cr,2}} \tag{23}$$

## 4. Examples

Comparing the presented out-of-plane instability proposal to the geometric equivalent imperfection for bending and compression can solve four examples. Current Eurocode, GMNIA (geometric and material nonlinear analysis of the imperfect structure) and the test results can be compared by discussing the factors that influence differences.

Applying the Beamcolumnimperfection software by Agüero [15] provides the plots below:

**Plot 1:** v (lateral displacement), $\theta_x$ (torsional rotation), $M_z$ (bending moment around a weak axis), B (Bimoment).

**Plot 2:** Utilization $M_z$, B, My (bending moment around a strong axis), N (axial force) and a linear interaction formula.

**Plot 3:** $T_t$ (Saint-Venant Torsional moment), $T_w$ (Warping torsional moment), $V_y$ (shear force that parallels axis y), $V_z$ (Shear force that parallels axis z).

Plasticity is considered concentrated by means of a simplified linear interaction equation or with exact curves obtained by linear programming (simplex).

The number of elements used for beams and columns is 20.

In the portal frame, warping is considered continuous in the beam-column connection.

### *4.1. Example 1*

The beam with IPE 200, S235 (Figs. 1-3) is studied with fork supports (3.78 m long), compression force and concentrated force at the midspan. The impact of the midspan load application on the shear center and top flange is examined, and the obtained results are compared to GMNIA Papp [13].

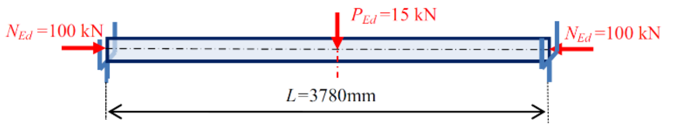


**Fig. 1** Example of a figure

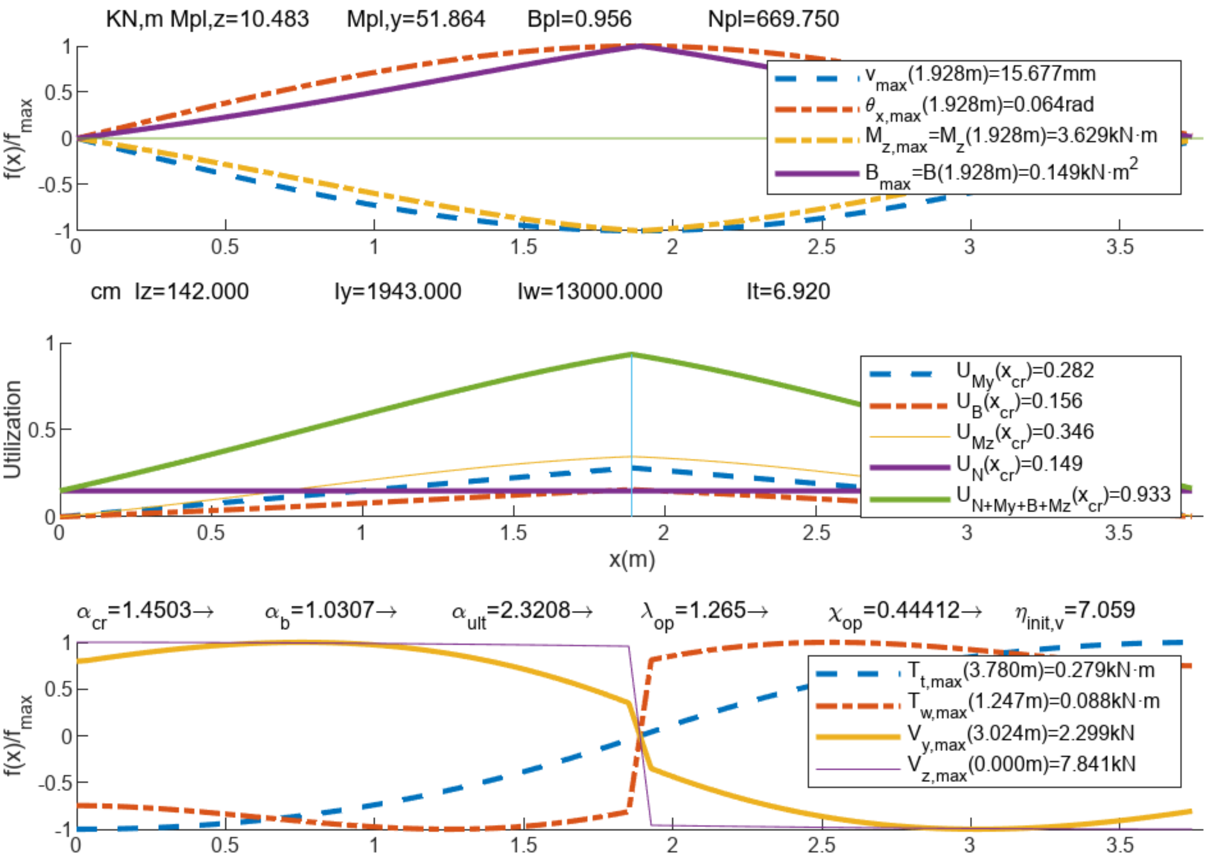


**Fig. 2** Example 1: $P_{Ed}$ is applied to the top flange of IPE 200, S235

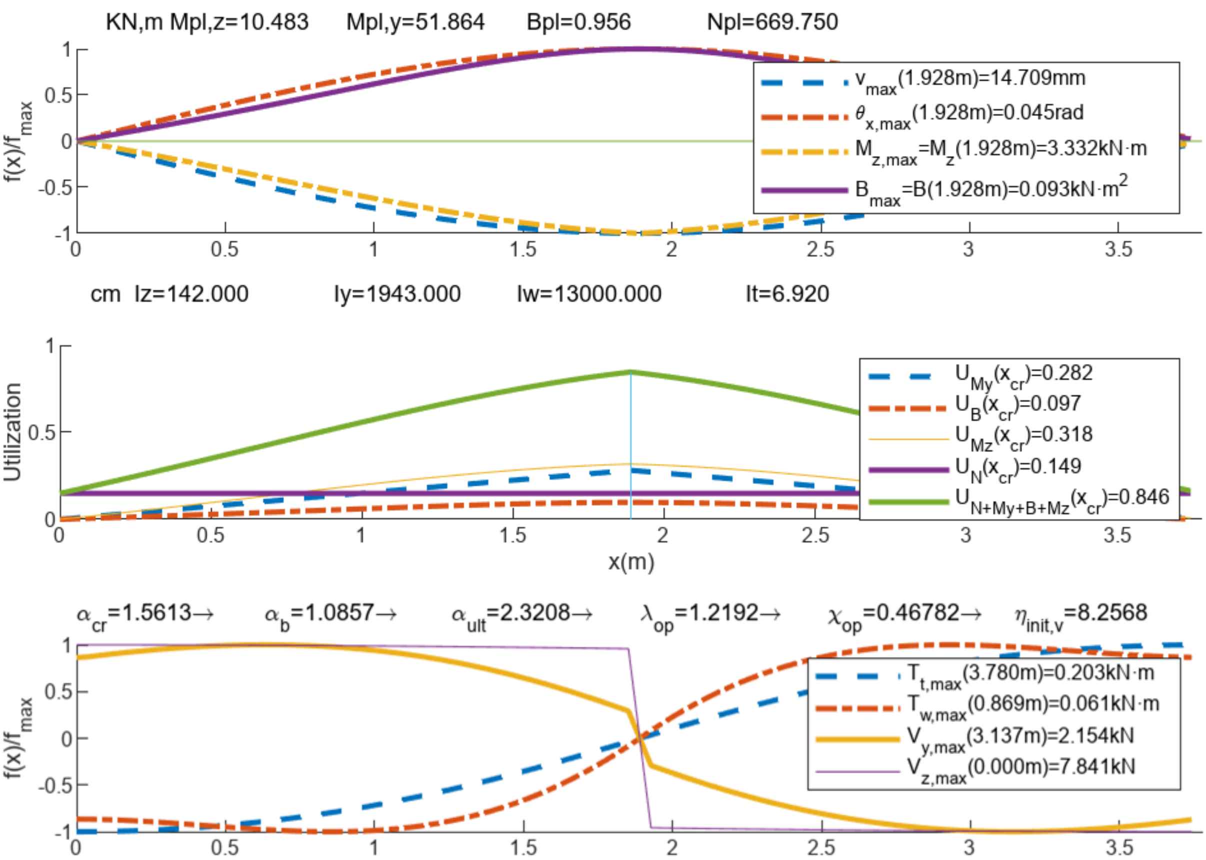


**Fig. 3** Example 1: $P_{Ed}$ is applied to the shear center of IPE 200, S235

*4.2. Example 2*

The beam with IPE 500, S235 (Figs. 4 to 10) is examined with not only fork supports (8.097 m long), but also the lateral support on the top flange at the midspan. A moment is applied to one support and compression force. The compression and bending moment combination is studied, and leads to failure in this example. The GMNIA results and those in Papp [13] are compared.

In example 2, the lateral support at the midspan is located on the top flange. The compression-bending moment combination fails.

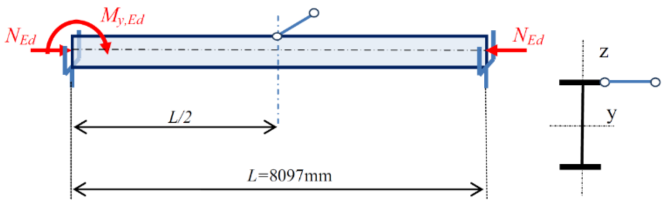


**Fig. 4** Example 2: geometry and loadings IPE 500, S235

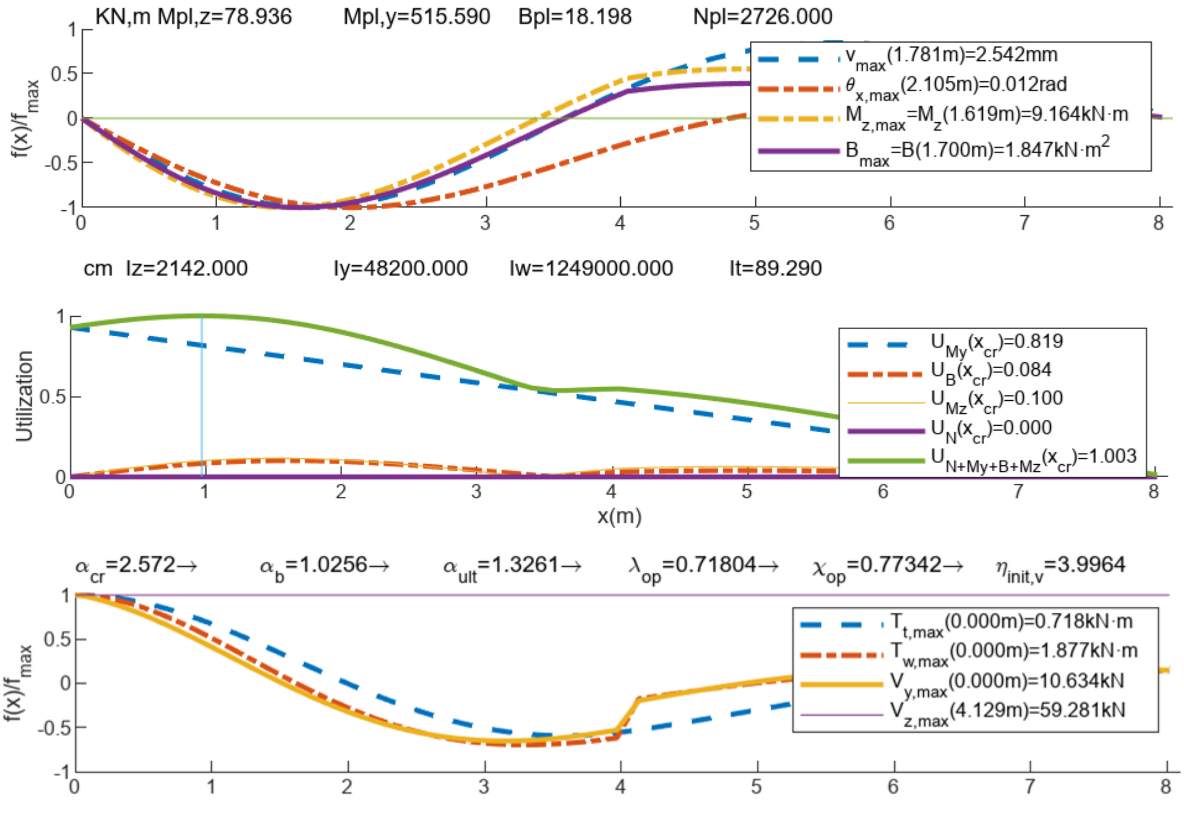


**Fig. 5** Example 2a: Combination of N = 0 kN, My = 480 kNm

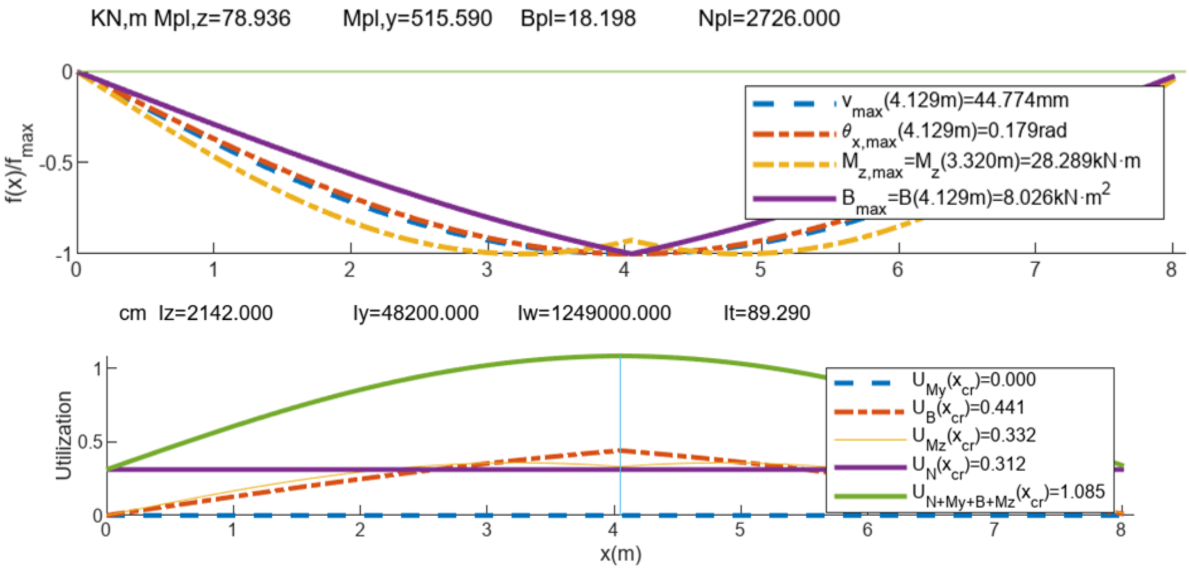

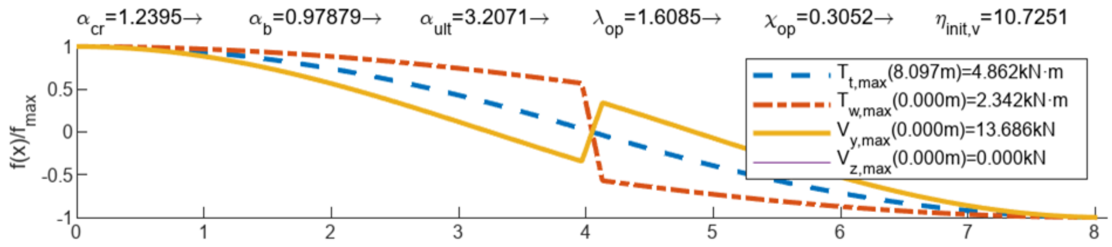


**Fig. 6** Example 2b: Combination of N = 850 kN, My = 0 kNm

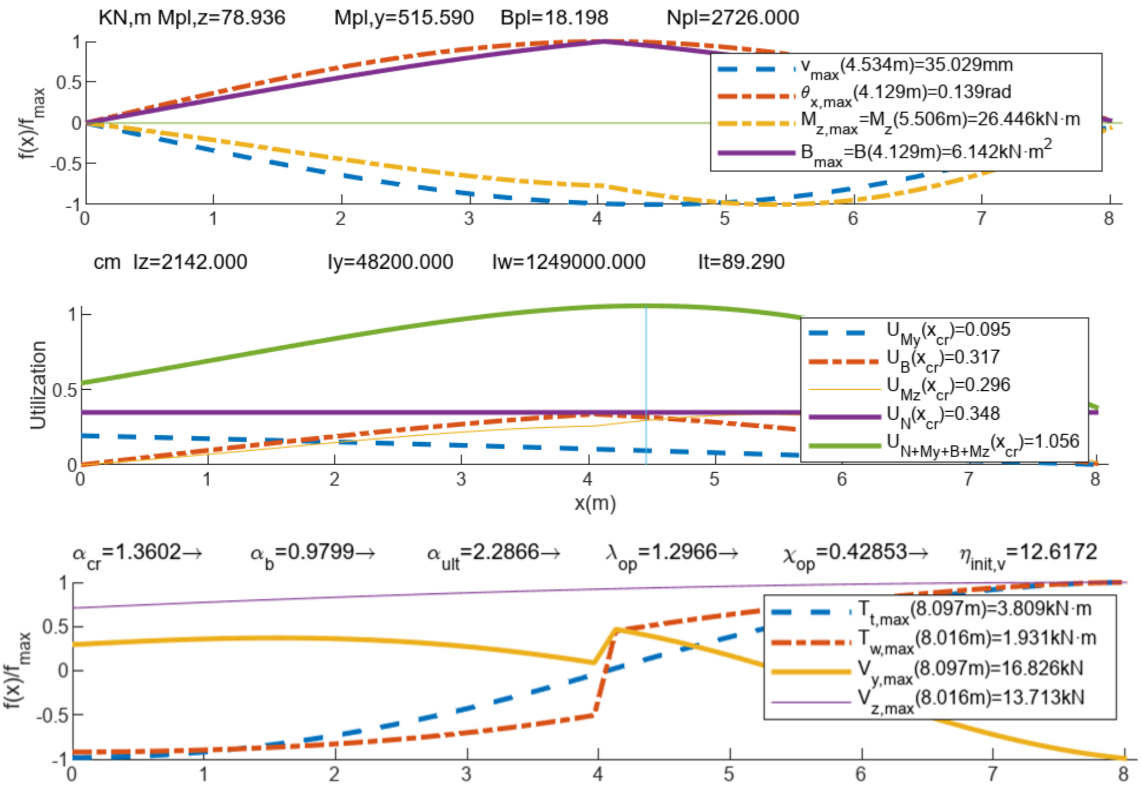


**Fig. 7** Example 2c: Combination of N = 950 kN, My = 100 kNm

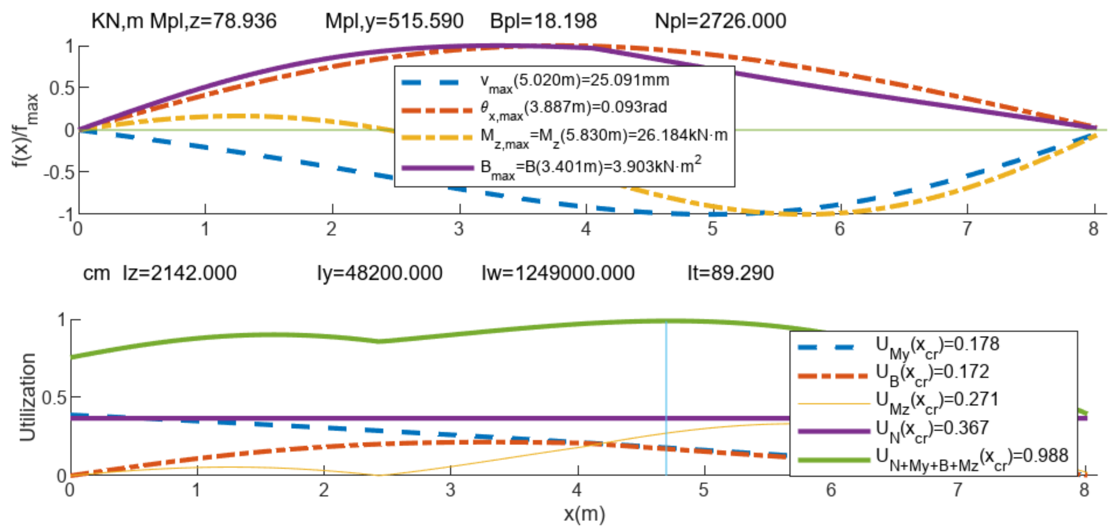

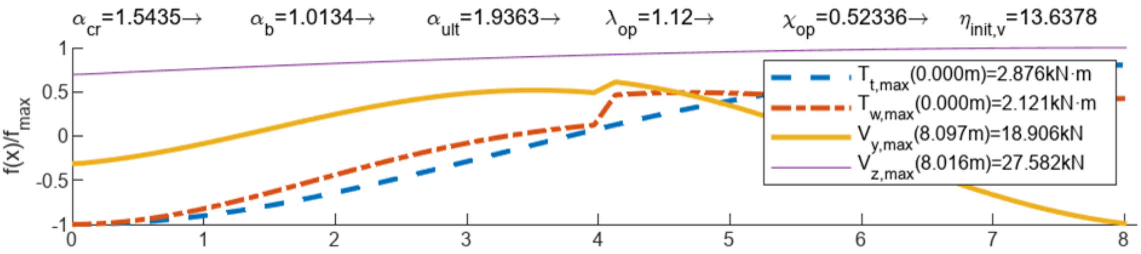


**Fig. 8** Example 2d: Combination of N = 10000 kN, M y = 200 kNm

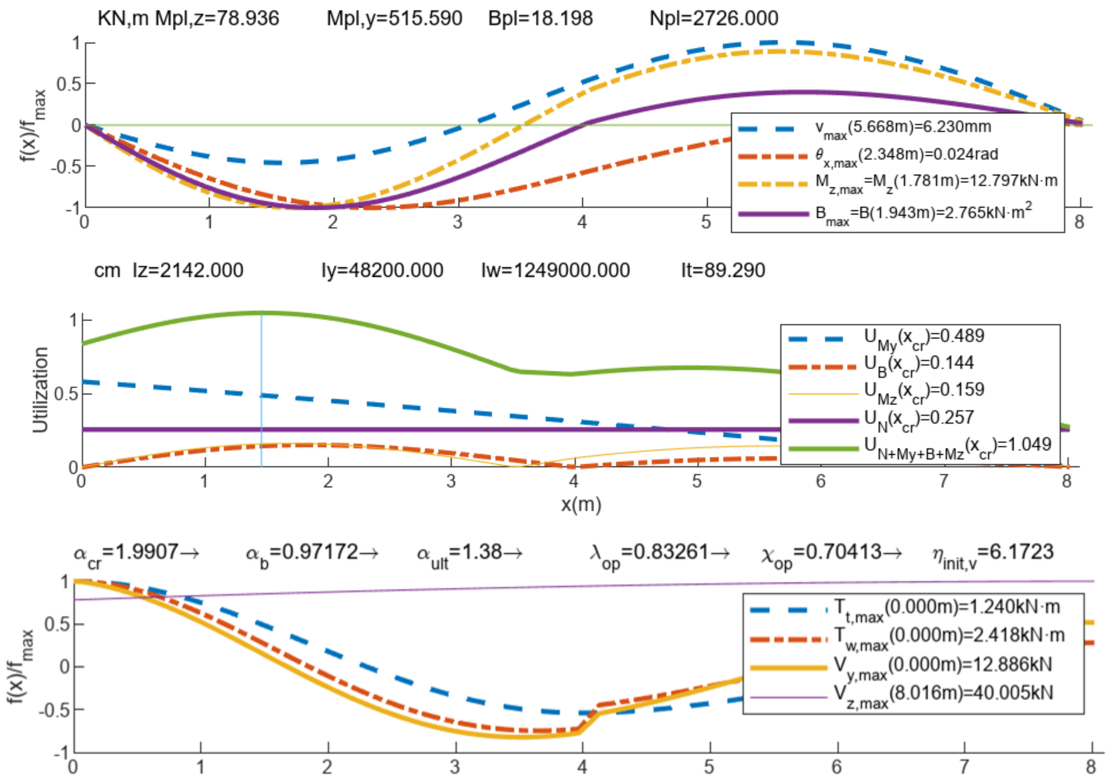


**Fig. 9** Example 2e: Combination of N = 700 kN, My = 300 kNm

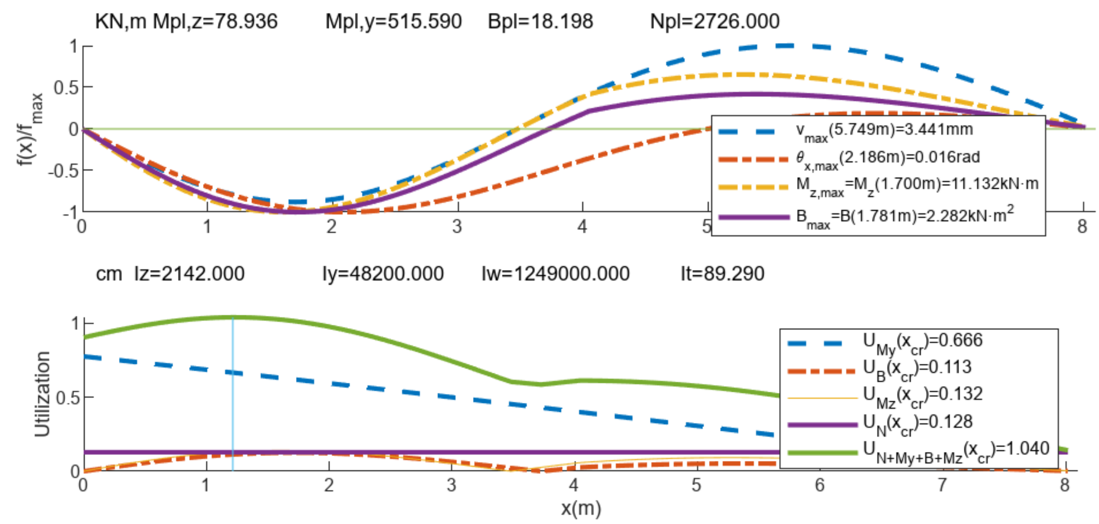

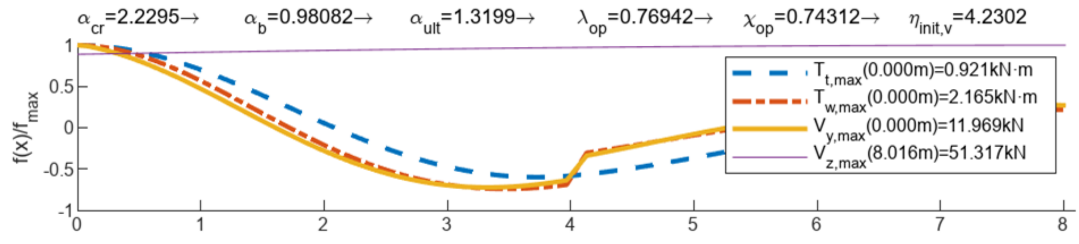


**Fig. 10** Example 2f: Combination of N = 350 kN, My = 400 kNm

### *4.3. Example 3*

Work is done with the beam by applying HEB 200, fy = 378 MPa (Figs. 11-15) and fork supports (7.8 m beam column length). Compression force + eccentric load applied at the midspan. Eccentricity is $e_y$=100 mm, $e_z$=-150 mm. The obtained results and the experimental ones reported in Winkler et al. [16] are compared. Two assumptions apply to solve this example with: warping-free on supports; restrained warping.

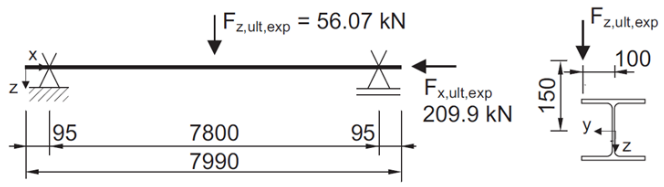


**Fig. 11** Example 3: geometry and loadings. HEB 200, $f_y$ = 378 Mpa

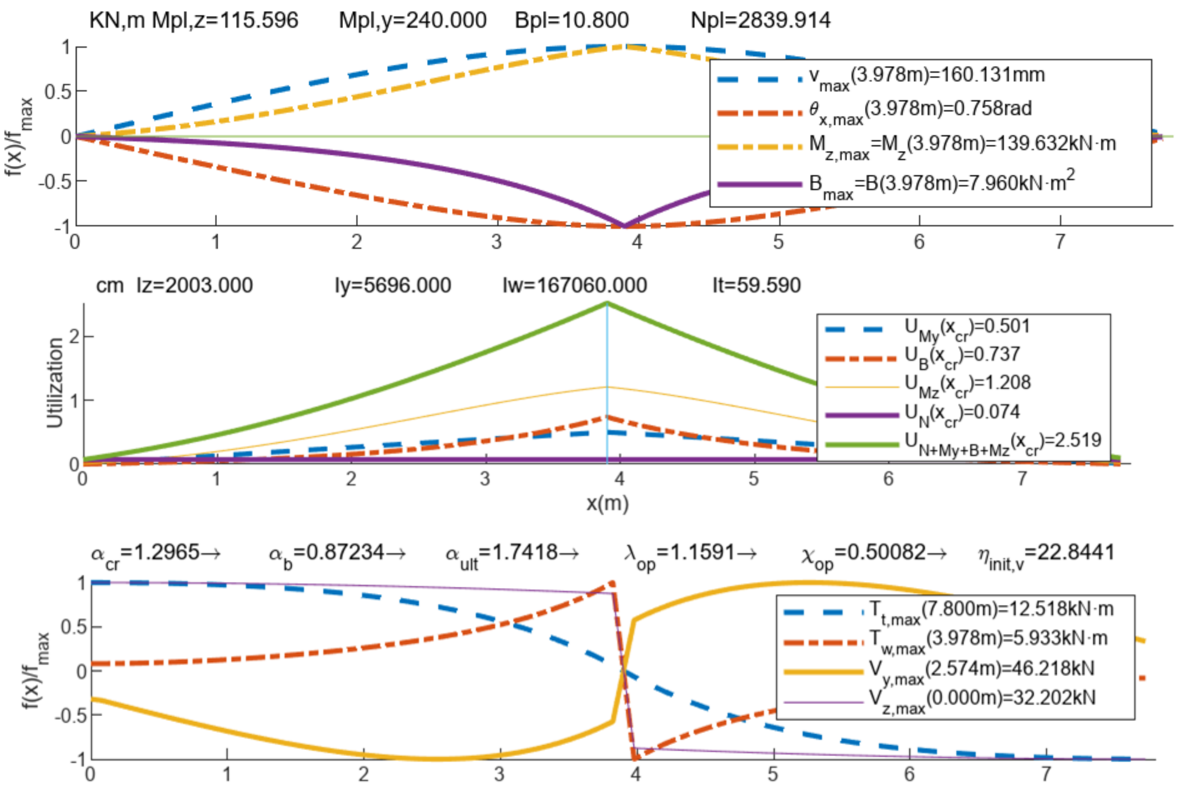


**Fig. 12** Example 3: it considers the maximum experimental load and a linear interaction formula

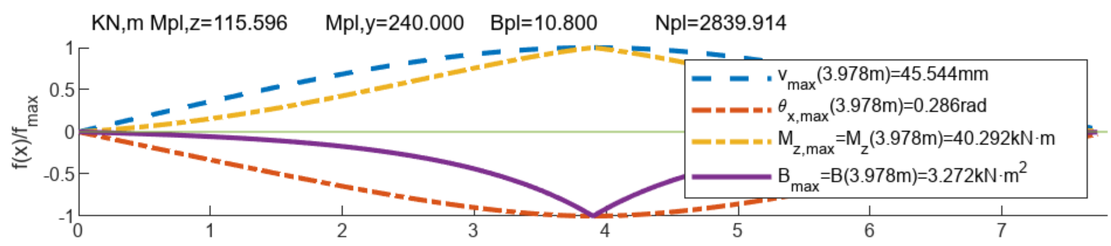

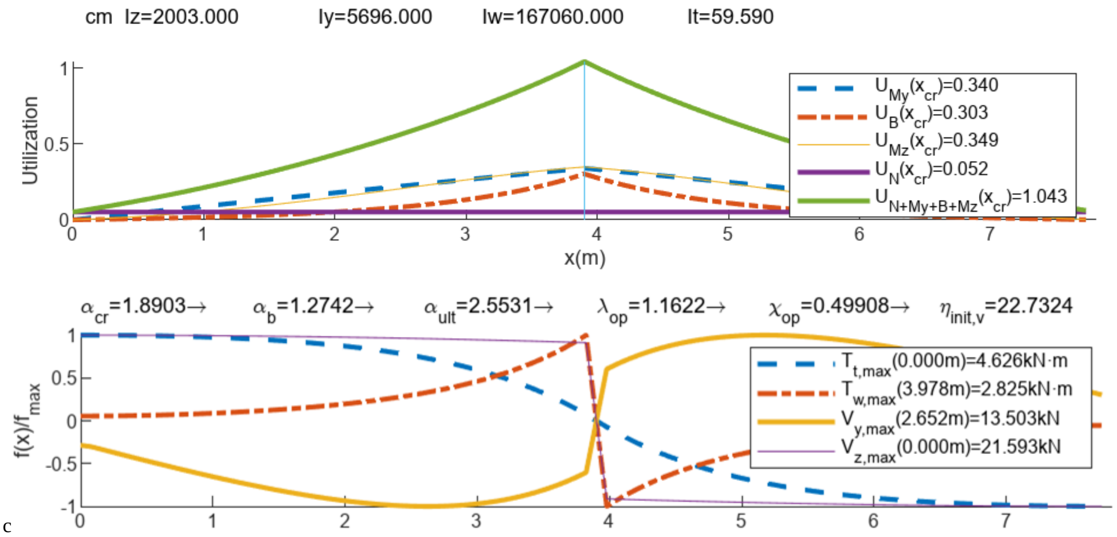


c

**Fig. 13** Example 3: it considers a 70% maximum experimental load and a linear interaction formula

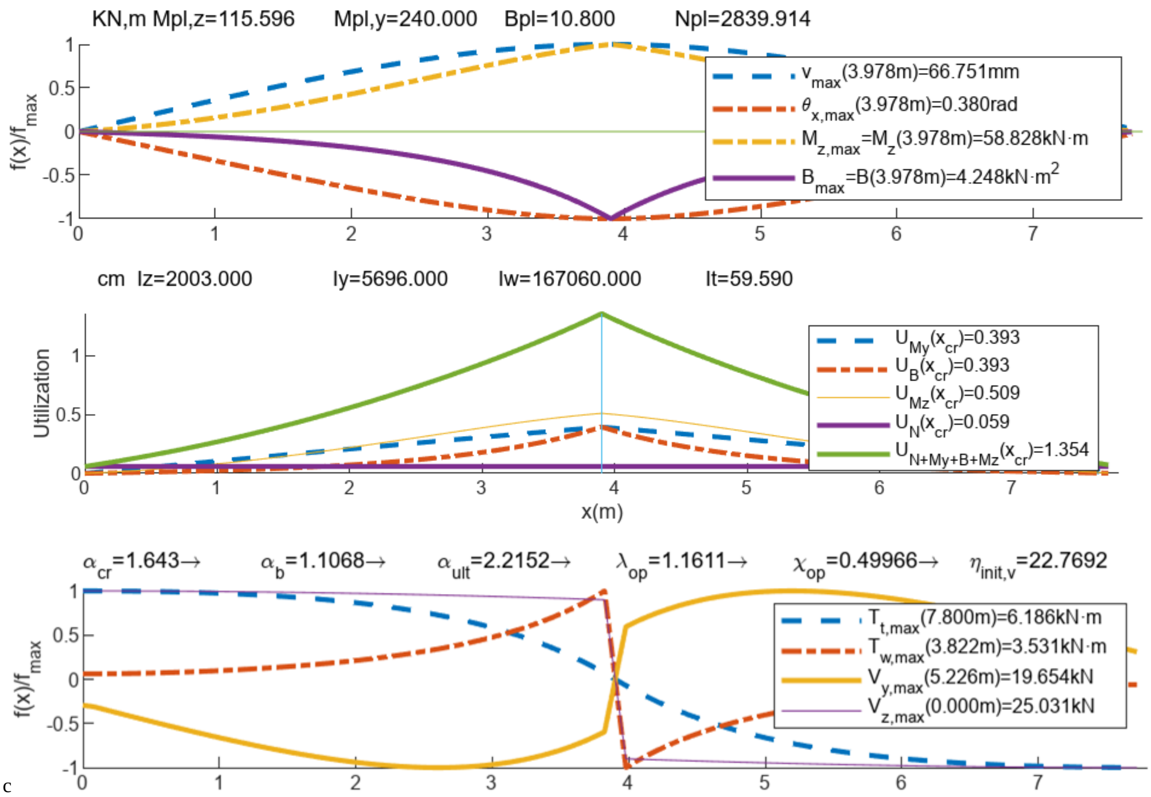


c

**Fig. 14** Example 3: it considers an 80% maximum experimental load and a linear interaction formula with the linear interaction formula utilization factor U = 1.354 with the Thinwallsectiongeneral software by Agüero [16][1]

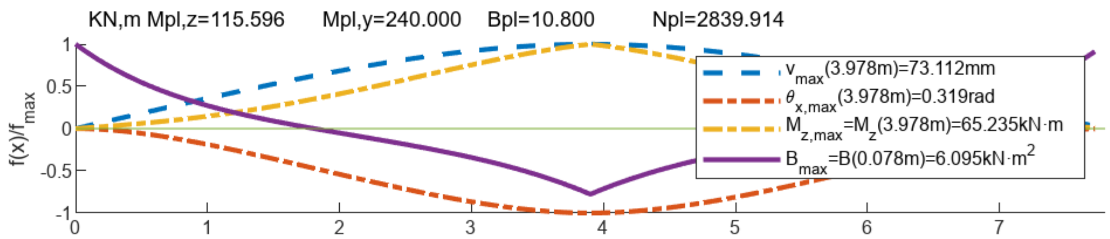


[1] A real interaction formula results in utilization factor U = 1/1.052 = 0.95. By including out-of-plane imperfection, the ultimate load exceeds the 80% load achieved with the experimental results, and material hardening is also taken into account

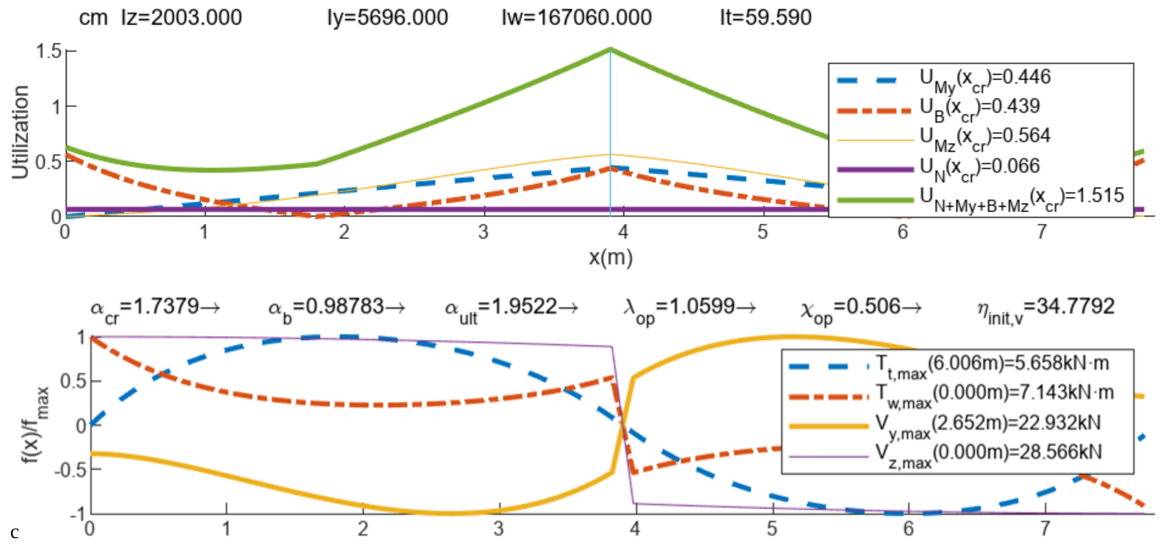


**Fig. 15** Example 3: it applies a 90% ultimate load and warping is taken as restrained. The utilization factor with a linear interaction formula is U = 1.515, but is 1.06 $\approx$ 1.0 when the real interaction is taken into account with the Thinwallsectiongeneral software [16].

### *4.4. Portal frame components*

The portal frame (Figs. 16-19) is computed by Chladný's UGLI imperfection method. During calculations, safety factor $\gamma_{M1}$ = 1.1 in quantity $e_{0,m}$ is employed. This is set out in EN 1999-1-1:2023, EN 1999-1-1:2007 and EN 1993-1-1:2005. Safety factor $\gamma_{M1}$ in EN 1993-1-1:2022 lacks $e_{0,m}$. Fig.17a and Fig.17b contain the obtained outcomes.

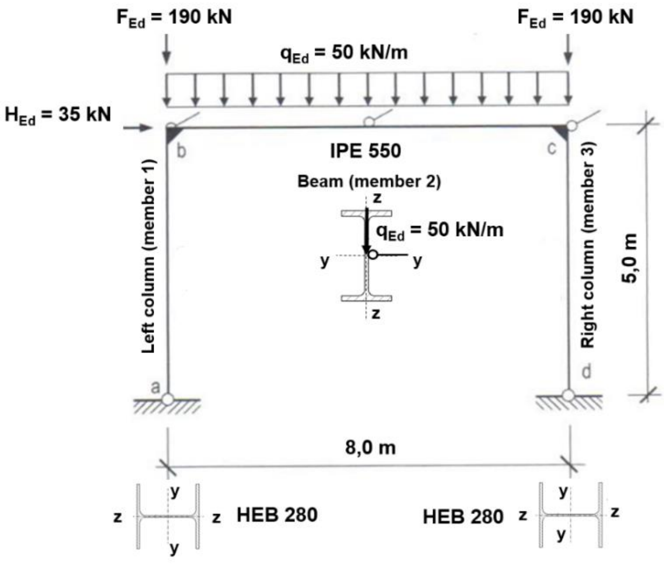


**Fig. 16** Investigated portal frame

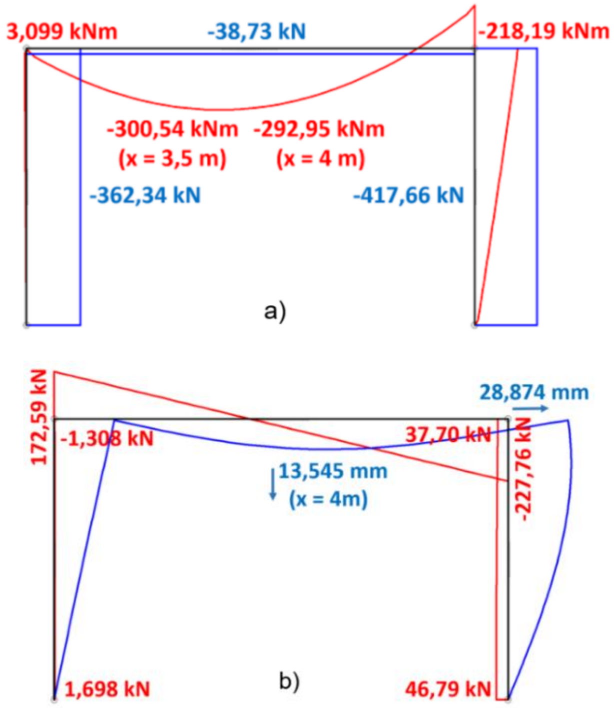


**Fig. 17** (a) Distribution of bending moments and normal force; (b) distribution of shear forces and deformation of the investigated portal frame due to UGLI imperfection

Applying clause 8.3.3 "Uniform members in bending and axial compression" of EN 1993-1-1:2022, which include interaction formulae (8.88) and (8.89), results in the internal forces that appear in Fig. 17, as well as these utilization factors: a) U = 0.850 for the right column; b) U = 0.653 for the left beam part (Fig. 16).

Examples 4.4a and 4.4b investigate the beam and right column as individual members that are loaded by normal forces, end moments and uniform loading q to generate exactly the same internal forces as those found in Fig. 17. The impact that the out-of-plane UGLI imperfection of both the column (example 4.4a) and beam (example 4.4b) has on this portal frame components' behavior and their utilization factors is studied. A comparison is made of the utilization factors to the above values of 0.850 and 0.653, respectively, for the column and beam.

#### *4.4.a. Portal frame column*

If the column resistance verification is carried out in line with clause 8.3.3 of EN 1993-1-1:2022, it should be substituted for the calculation in Fig. 18. Hence the utilization factor would be 0.817 rather than 0.850. Indeed these differing procedures are not completely comparable.

#### *4.4.b. Portal frame beam*

If column resistance verification is performed as in clause 8.3.3 of EN 1993-1-1:2022, it would be substituted for the calculation in Fig. 19. The utilization factor would be 0.596 rather than 0.653. Indeed these differing procedures are not completely comparable.

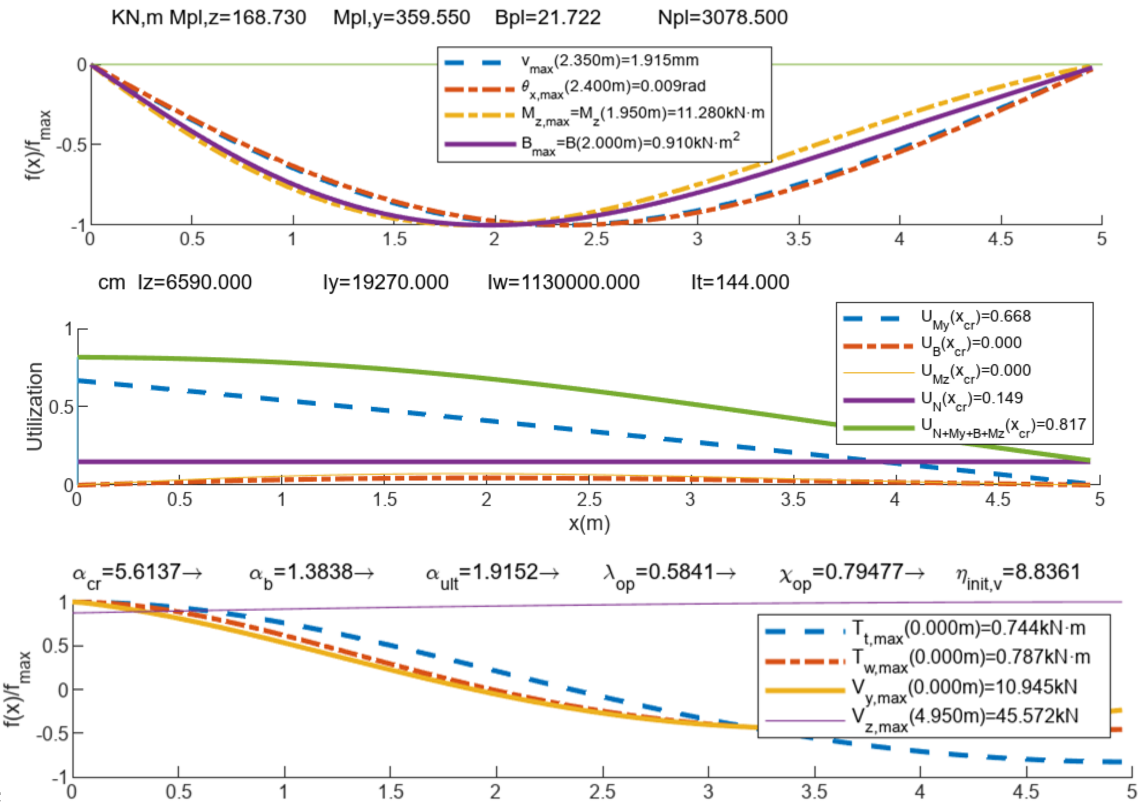


**Fig. 18** Example 4.4a: Column. HEB 280. Safety factor $\gamma_{M1}$ = 1.1 and imperfection factor $\alpha$ = 0.49. The utilization factor is U = 0.817

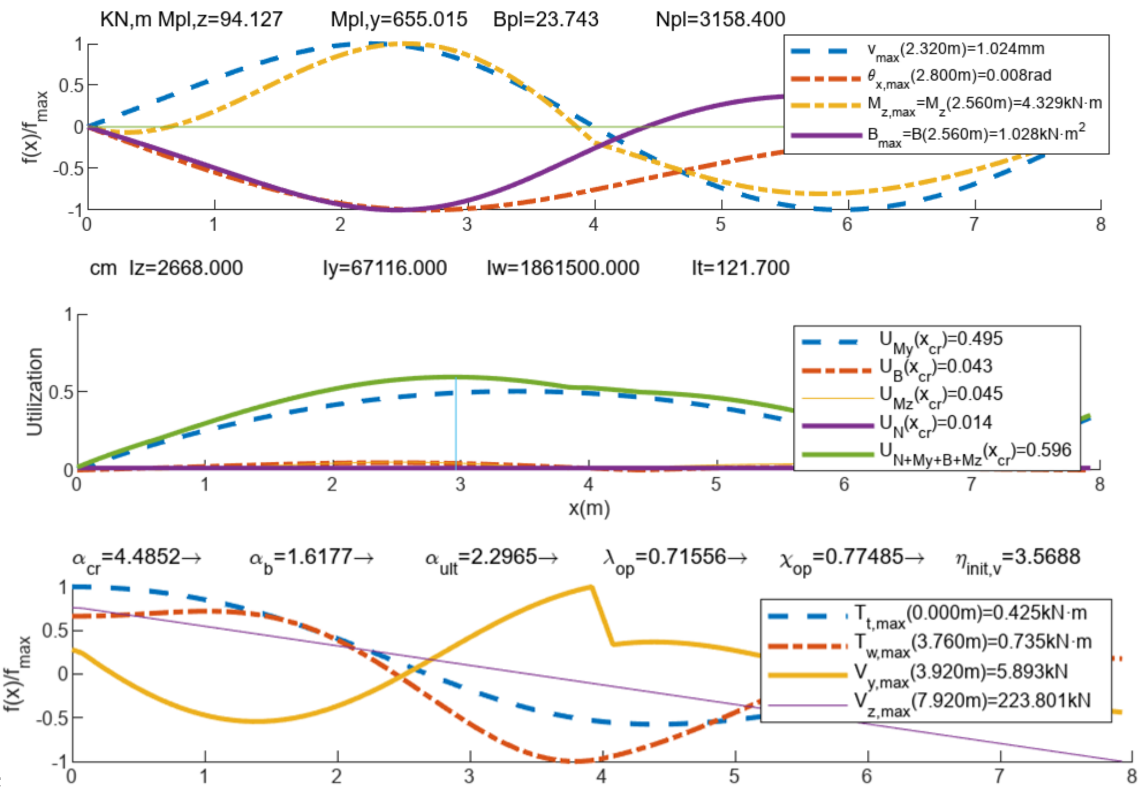


**Fig. 19** Example 4.4b: Beam. IPE 550. Safety factor $\gamma_{M1}$ = 1.1 and imperfection factor $\alpha$ = 0.34. The utilization factor is U = 0.596

## 5. Comparisons to other authors and GMNIA

Example 1 (Figs. 1 to 3) and Example 2 (Figs. 4 to 10) show results that compare to those in Papp [13].

Example 1 indicates that the utilization factor in accordance with GMNIA is U = 0.89, and is U = 0.933 in accordance with this proposal when the load application point is on the top flange surface, and U = 0.846 when load acts in the shear center. Further information can be found in Papp's article in Example 6, Table 6.

Example 2 shows how our results are on the safe side by 10% vs. those indicated by GMNIA. Further information can be found in Papp's article in Example 7, Fig. 11.

Example 3 (Figs. 11 to 15) contains results that are comparable to Winkler et al. [17]. Our results are on the safe side vs. the experimental results.

If the beam end cross-sections on supports are warping-free, our results are on the safe side by 20% vs. the test results. If warping is constrained at beam ends, our results are also on the safe side by 10% vs. the test results.

Example 4 is compared to the Eurocode method [18] for designing beam-columns after investigating portal frame components: beam (Example 4.4a); column (Example 4.4b). Comparisons appear in relation to the: (i) results in line with interaction formulae (8.88) and (8.89) in [3]; (ii) results acquired according to the herein proposed procedure.

## 6. Conclusions

A generalization of Chladný's method is proposed to explain buckling resistance in sensitive structures to flexural buckling. This method falls in line with the former generalizations to lateral torsion owing to bending and flexural torsional buckling given compression. In the present work, the proposed imperfection is utilized in out-of-plane owing to compression-bending with the reference clause 6.3.4 in [1,2] or 8.3.4 in [3].

Five examples are employed to compare the method. It offers good agreements with the GMNIA, test and Eurocode 3 design proposals.

Our method is also applied in four examples: example 1 (Figs. 1-3); example 2 (Figs. 4-10); example 3 (Figs. 11-15); example 4 (Figs. 16-20). Comparisons are made to Papp [13] by employing GMNIA (examples 1 and 2), the test of Winkler et al. [17] (example 3) and the Eurocode procedure [18] (example 4), and all with acceptable agreements.

### Appendix. Nomenclature

$\alpha$ denotes the imperfection factor related to the flexural buckling curve (Tables 6.1 and 6.2 in EN 1993-1-1 [1]; Tables 3.2 and 6.6 of EN 1999-1-1 [2])

$\alpha_{LT}$ represents the imperfection factor for lateral torsional buckling related to the buckling curve (Tables 6.3, 6.4 and 6.5 of EN 1993-1-1 [1]; 6.3.2.2 of EN 1999-1-1 [2])

$\alpha_{cr}$ depicts the minimum load amplifier for axial force configurations in members to achieve elastic critical buckling loads (5.2.1(3) of [1]; 5.2.1(3) of [2])

$\alpha_{ult}$ refers to the amplifier for members' load to accomplish critical cross-section resistance (6.3.4(2) in [1]. A more convenient symbol αult,k is utilized; [2] is unaware of this quantity/symbol)

$\alpha_b$ relates to relative lateral torsional buckling resistance (Eq. 12); [1] and [2] do not employ the symbol)

$\gamma_{M0}$ indicates the partial safety factor for cross-section resistance when the Class cross-section is (6.1 in [1]; [2] is unaware of such quantity/symbol)

$\gamma_{M1}$ refers to the partial safety factor for members that resist instability, evaluated by member checks (6.1 of [1] and 6.1.3; Table 6.1 of [2])

$\chi$ denotes the reduction factor for the relevant buckling curve (6.3.1.2 of [1]; 6.3.1.2 of [2]

$\chi_{LT}$ depicts the reduction factor for lateral torsional buckling in relation to relative slenderness (6.3.1.2 of [1]; 6.3.1.2 of [2])

$\bar{\lambda}$ indicates the plateau length of buckling curves (for steel [1]: 0.2; for aluminum alloy [2]: 0.1 for Buckling Class A, 0.0 for Buckling Class B)

$\bar{\lambda}_0$ denotes relative slenderness for lateral torsional buckling (6.3.2.2 and 6.3.2.3 of [1]; 6.3.2.2 of [2])

$\bar{\lambda}_{LT}$ represents the plateau length for lateral torsional buckling curves (for steel [1]: 0.2 of 6.3.2.2 and 0.2-0.4 of 6.3.2.3; for aluminum alloy [2]: 0.6 for Class 1 and 2 cross-sections; 0.4 for Class 3 and 4 cross-sections of 6.3.2.2)

$\bar{\lambda}_{op}$ refers to the relative slenderness for out-of-plane buckling (6.3.4 of [1] and [2])

$\beta$ denotes the correction factor for lateral torsional buckling curves (6.3.2.3 in [1]; [2] is unaware of this quantity/symbol)

$\{\eta_{init}\}$ indicates UGLI imperfection in the elastic critical buckling mode shape

$\{\eta_{cr}\}$ identifies the elastic critical buckling mode shape

$\eta_{cr,w}$ depicts buckling shape component displacement perpendicularly to axis y

$\eta_{cr,v}$ depicts buckling shape component displacement perpendicularly to axis z

$\eta_{cr,\theta x}$ is related to the torsional rotation of the buckling shape component around the shear center axis

A means the cross-sectional area

$\eta_0$ denotes UGLI imperfection amplitude

E stands for the modulus of elasticity (210 000 MPa for steel [1]; 70 000 MPa for aluminum alloy [2])

$I_y$, $I_z$ respectively reflect the second moments of the area in relation to axes y and z

$I_w$ denotes the warping constant

$N_{cr}$ implies the elastic critical force of the relevant buckling mode in accordance with gross cross-section properties

$M_{y,Ed}$ represents the design value for the bending moment around axis y

$N_{Rk}$ reflects the characteristic resistance of normal force on critical section $x_{cr}$

$M_{Rk}$ denotes the characteristic resistance of the bending moment on critical section $x_{cr}$

$U_{N+My+Mz+B}$ respectively indicate the utilization factor given by $N_{Ed}$, $M_{y,Ed}$, $M_{z,Ed}$, and $B_{Ed}$

$W_z$ represents the section modulus around axis z

$W_y$ represents the section modulus around axis y

$W_B$ means the warping section modulus

$x_{cr}$ depicts the critical section; the utilization factor is higher than the factors in all the other sections

### Appendix. Background equations to analyze the imperfect structure.

The following equation is used to perform the analysis of the imperfect structure; these equations are implemented in the software ¨Buckling Beam Column N My Mz B T any support & section¨ by Aguero [19,20]. Other software can be found in [21]:

$$\left(\left[K_L\right]+\left[K_G\right]\right)\{d\}=\{f_{ext}\}+\left[K_G\right]\{\eta_{init}\} \tag{24}$$

Where:

$$\left[K_L\right]\{d\}\leftarrow\frac{1}{2}\int_0^L\left(EA\left(\frac{du}{dx}\right)^2+GJ\left(\frac{d\theta_x}{dx}\right)^2+EI_y\left(\frac{d^2w}{dx^2}\right)^2+EI_z\left(\frac{d^2v}{dx^2}\right)^2+EI_w\left(\frac{d^2\theta_x}{dx^2}\right)^2\right)dx \tag{25}$$

$$\left[K_G\right]\{d\}\leftarrow\frac{1}{2}\int_0^L\left(\begin{array}{l}N\left[\left(\frac{dv}{dx}\right)^2+\left(\frac{dw}{dx}\right)^2+2z_{sc}\left(\frac{dv}{dx}\right)\left(\frac{d\theta_x}{dx}\right)-2y_{sc}\left(\frac{dw}{dx}\right)\left(\frac{d\theta_x}{dx}\right)+\left(\frac{d\theta_x}{dx}\right)^2r_0^2\right]\\+2M_z\left(\frac{d^2w}{dx^2}\right)\left(\frac{d\theta_x}{dx}\right)+2M_y\left(\frac{d^2v}{dx^2}\right)\left(\frac{d\theta_x}{dx}\right)+\left(M_y\beta_z-M_z\beta_y+B\beta_w\right)\left(\frac{d^2\theta_x}{dx^2}\right)^2\end{array}\right)dx \tag{26}$$

$$\begin{aligned}\beta_z&=\frac{1}{I_y}\iint z\left(y^2+z^2\right)dA-2z_{sc}\\\beta_y&=\frac{1}{I_z}\iint y\left(y^2+z^2\right)dA-2y_{sc}\\\beta_w&=\frac{1}{I_w}\iint w\left(y^2+z^2\right)dA\\r_0^2&=\frac{I_y+I_z}{A}+y_{sc}^2+z_{sc}^2\end{aligned} \tag{27}$$

**Funding**

This research project is supported by the Slovak Grant Agency VEGA No.1/0155/23.

**References**

[1] Eurocode 3: Design of steel structures. Part 1.1: General rules and rules for buildings. EN 1993-1-1, 2005, Corrigendum AC, 2006, Corrigendum AC, 2009, Amendment A1, 2014, CEN Brussels.

[2] Eurocode 9: Design of aluminium structures.Part 1.1: General structural rules. EN 1999-1-1, 2007, Amendment A1, 2009, Amendment A2, 2013, CEN Brussels.

[3] Eurocode 3: Design of steel structures. Part 1.1: General rules and rules for buildings. EN 1993-1-1, 2022, CEN Brussels.

[4] Eurocode 9: Design of aluminium structures. Part 1.1: General structural rules. prEN 1999-1-1, 2020-07-01, CEN Brussels.

[5] E. Chladný and M. Štujberová, Frames with unique global and local imperfection in the shape of the elastic buckling mode (part 1), Stahlbau, 8, pp. 609-617, 2013.

[6] E. Chladný and M. Štujberová, Frames with unique global and local imperfection in the shape of the elastic buckling mode (Part 2), Stahlbau, 9, pp. 684-694, 2013.

[7] E. Chladný and M. Štujberová, Errata: frames with unique global and local imperfection in the shape of the elastic buckling mode. Part 1, Stahlbau, 82:H. 8, S. 609–617, 2013. Part 2. Stahlbau, 83:H. 9, S. 684–694, 2013. Stahlbau, 82:H. 9 S. 684-694, 2013. Stahlbau, 1, 64-64, 2014.

[8] I. Baláž, "Determination of the flexural buckling resistance of frames with members with non-uniform cross-section and non-uniform axial compression forces", Zborník z XXXIV Aktívu pracovníkov odboru OK so zahraničnou účast'ou "Teoretické a konštrukčné problémy ocel'ových a drevených konštruckcií a mostov", 16–17, 10, Pezinok, 17–22, 2008.

[9] A. Agüero, L. Pallarés and F.J. Pallarés, "Equivalent geometric imperfection definition in steel structures sensitive to flexural and/or torsional buckling due to compression", Engineering Structures, 96(1), 160-177, 2015.

[10] A. Agüero, F.J. Pallarés and L. Pallarés, "Equivalent geometric imperfection definition in steel structures sensitive to lateral torsional buckling due to bending moment", Engineering Structures, 96(1), 41-55, 2015.

[11] F. Bijlaard, M. Feldmann, J. Naumes and G. Sedlacek, "The "general method" for assessing the out of plane stability of structural members and frames and the comparison with alternative rules in EN1993 – Eurocode3 – Part 1-1", Steel Construction, 3(1), 19-33, 2010.

[12] M. Wieschollek, N. Schillo, M. Feldmann and G. Sedlacek. "Lateral–torsional buckling checks of steel frames using second-order analysis", Steel Construction, 5(2), 71-86, 2012.

[13] F. Papp, "Buckling assessment of steel members through overall imperfection method", Engineering Structures, 106, 124−136, 2016.

[14] N.S. Trahair, Flexural–torsional buckling of structures, E&Fnspon, 1993.

[15] A. Agüero, "Beamcolumnimperfection" Software, Online available from https://laboratoriosvirtuales.upv.es/webapps/Beamcolumn_imperfection.html, 2023

[16] A. Agüero, "Thinwallsectiongeneral" Software, Online available from https://laboratoriosvirtuales.upv.es/webapps/thinwallsectiongeneral.html, 2023.

[17] R. Winkler, A. Bours, A. Walter and M. Knobloch, "Redistribution of internal torsional moments caused by plastic yielding of structural steel members", Structures, 17, 21-33, 2019.

[18] I. Baláž, Manual to EN 1993-1-1:2022 with numerical examples in MATHCAD, ÚMS SR in Bratislava. In print.

[19] A. Agüero, "Buckling Beam Column N My Mz B T any support & section" Software, Online available from https://labmatlab-was.upv.es/webapps/home/Bucklingresistanceopenclosed_anyBC_N_My_Mz_B_U.html, 2023.

[20] A. Agüero. "Bucklingresistance open + closed" Software online available from: https://labmatlab-was.upv.es/webapps/home/Bucklingresistanceopenclosed.html, 2023

[21] A. Agüero. Software online https://antonioagueroramonllin.blogs.upv.es/, 2003